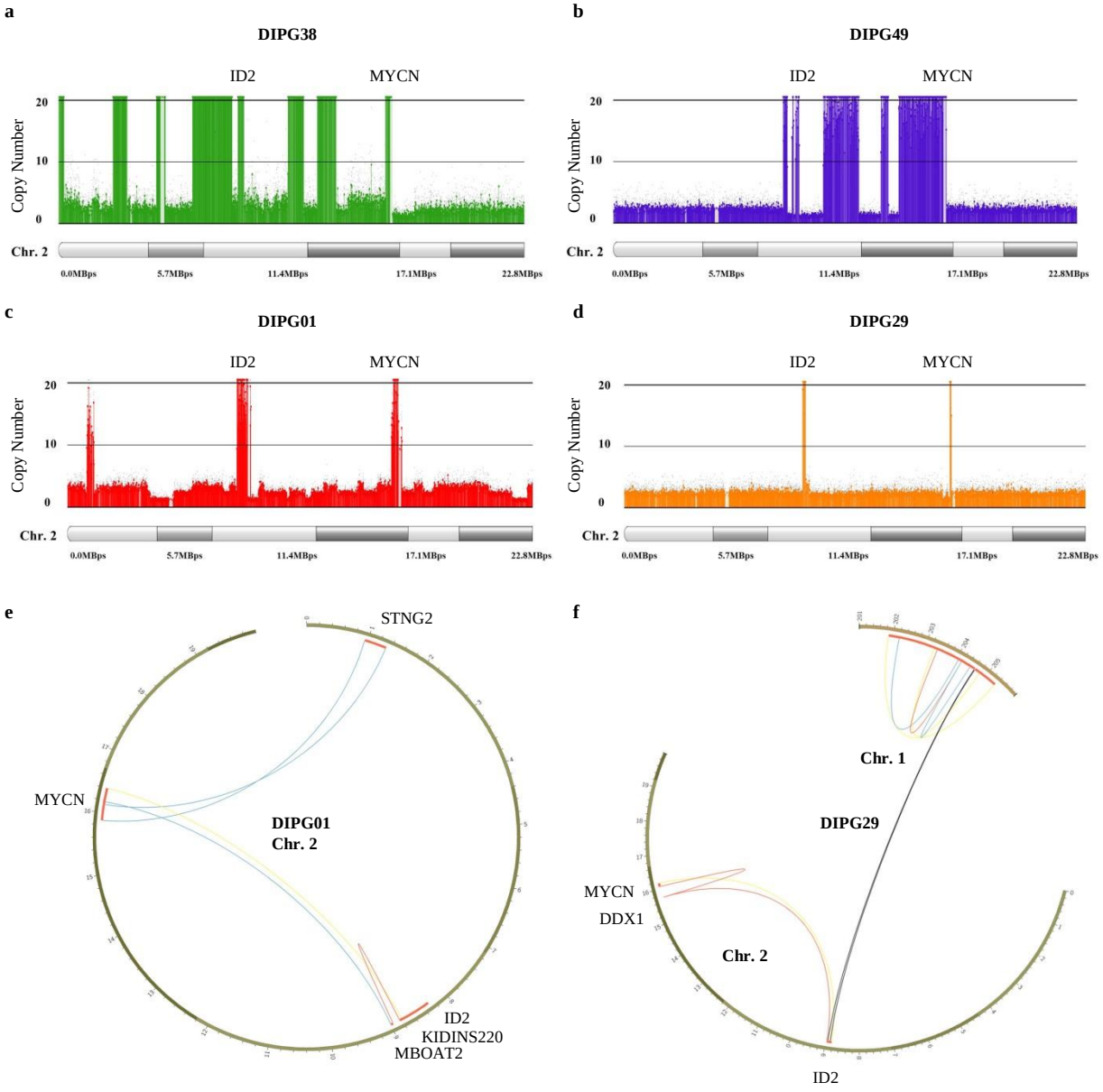

Supplementary Figure 1 MYCN subgroup show recurrent structural variants involving high level amplification and rearrangement of *MYCN*, *ID2* and *KIDINS220* on chromosome 2p. SNP6.0 copy number profiles of chromosome 2p focal, high-level amplifications in (a) DIPG38, (b) DIPG49, (c) DIPG01 and (d) DIPG29. These amplifications always involve the genes *MYCN*, *ID2* and *KIDINS220*. CIRCOS plots of structural variants in (e) DIPG01 and (f) DIPG29 as determine from WGS data.

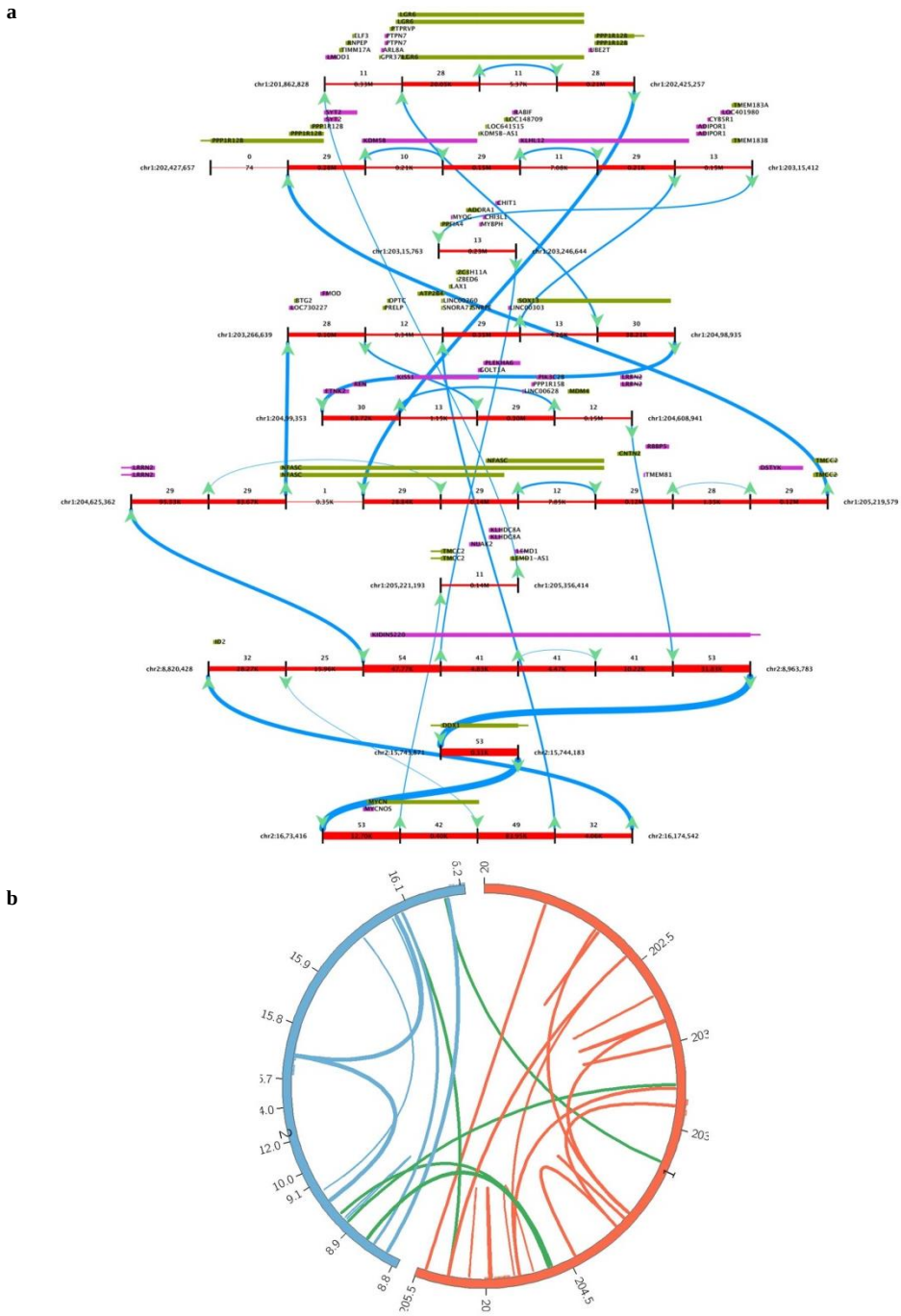

Supplementary Figure 2 Event graph and CIRCOS plot of chromothripsis in DIPG29. (a) The bi-directed event graph for a chromothripsis event in DIPG29. Red edges represent the genomic interval of their respective nodes. Blue edges represent groups of discordant read pairs supporting the same breakpoint. Arc width is proportional to the maximal likely copy count. (b) A CIRCOS plot of chromosome 1 and 2 from MYCN group patient, DIPG29. Only those clusters larger than 1000bp are shown between chr1 and chr2. The width of each arc is proportional to the log of its estimated copy count. The highest estimated copy count is 61.

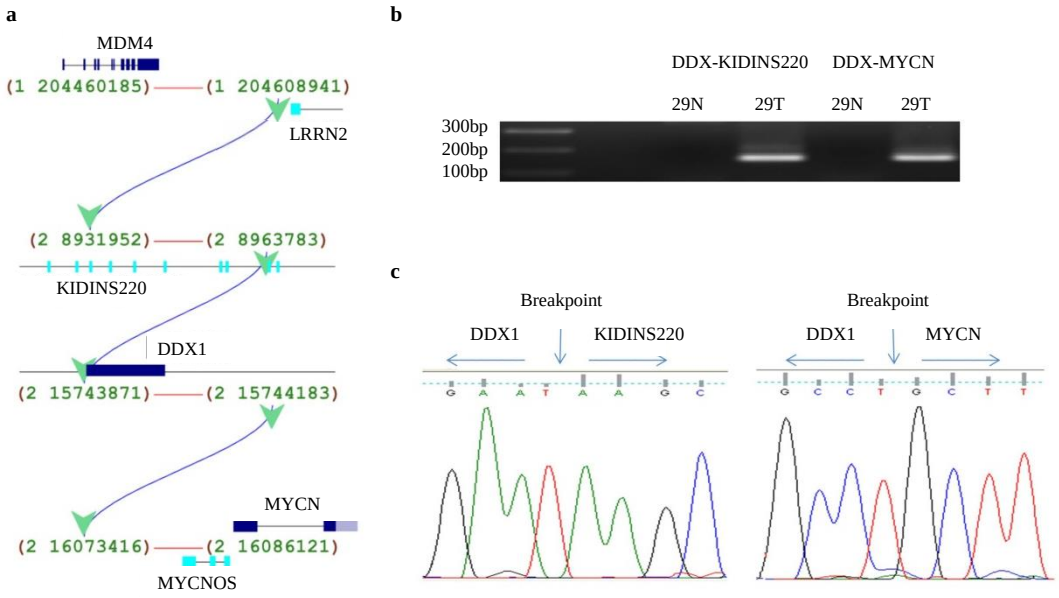

Supplementary Figure 3 Structural variant validation in DIPG29. (a) Structural variant spanning six breakpoints as predicted by discordant read-pair mappings in DIPG29. (b) PCR validation of *DDX1-KIDINS220* (Left primer: TCTATGCCAGTGCTTTACTCCTT; Right Primer: CTGTTCCACCAAAGCCAAAT) and *DDX1-MYCN* (Left Primer: TGAGCAGATTTTCTGTATATTTTCCA; Right Primer: GTCTCCCAGGCTGCAGTG) in tumour and matched normal show product band only in tumor DNA. (c) Sanger sequencing through breakpoints in *DDX1-KIDINS220* and *DDX1-MYCN* structural variants.

a

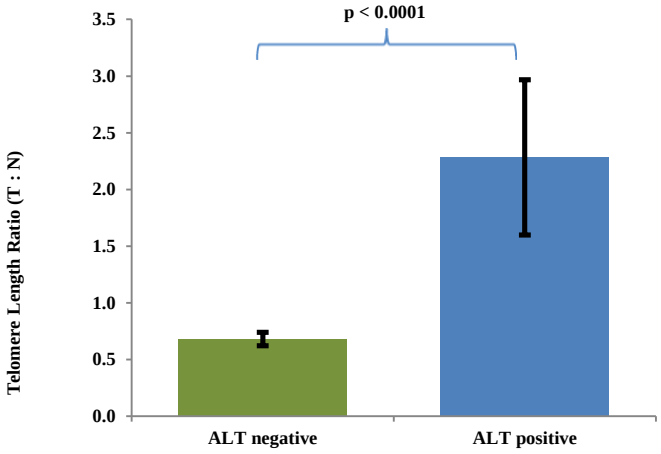

b

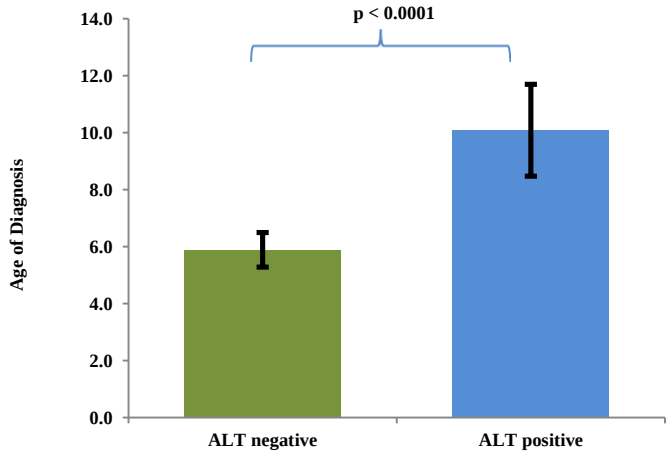

Supplementary Figure 4 DIPG patients with ALT phenotype have longer telomeres and are diagnosed at an older age. All ALT positive DIPG patients were found in the H3-K27M subgroup. By WGS, these patients had significantly longer telomeres; (a) 2.28 times longer than their matched normal vs. non-ALT DIPG patients which had telomeres that were 1.47 times shorter than their matched normal ($p < 0.0001$). (b) There was a significant difference in age of diagnosis between ALT negative (5.89 ± 2.82 years) vs. ALT positive (10.08 ± 3.61 years); $p < 0.0001$). Error bars represent the standard error of the mean.

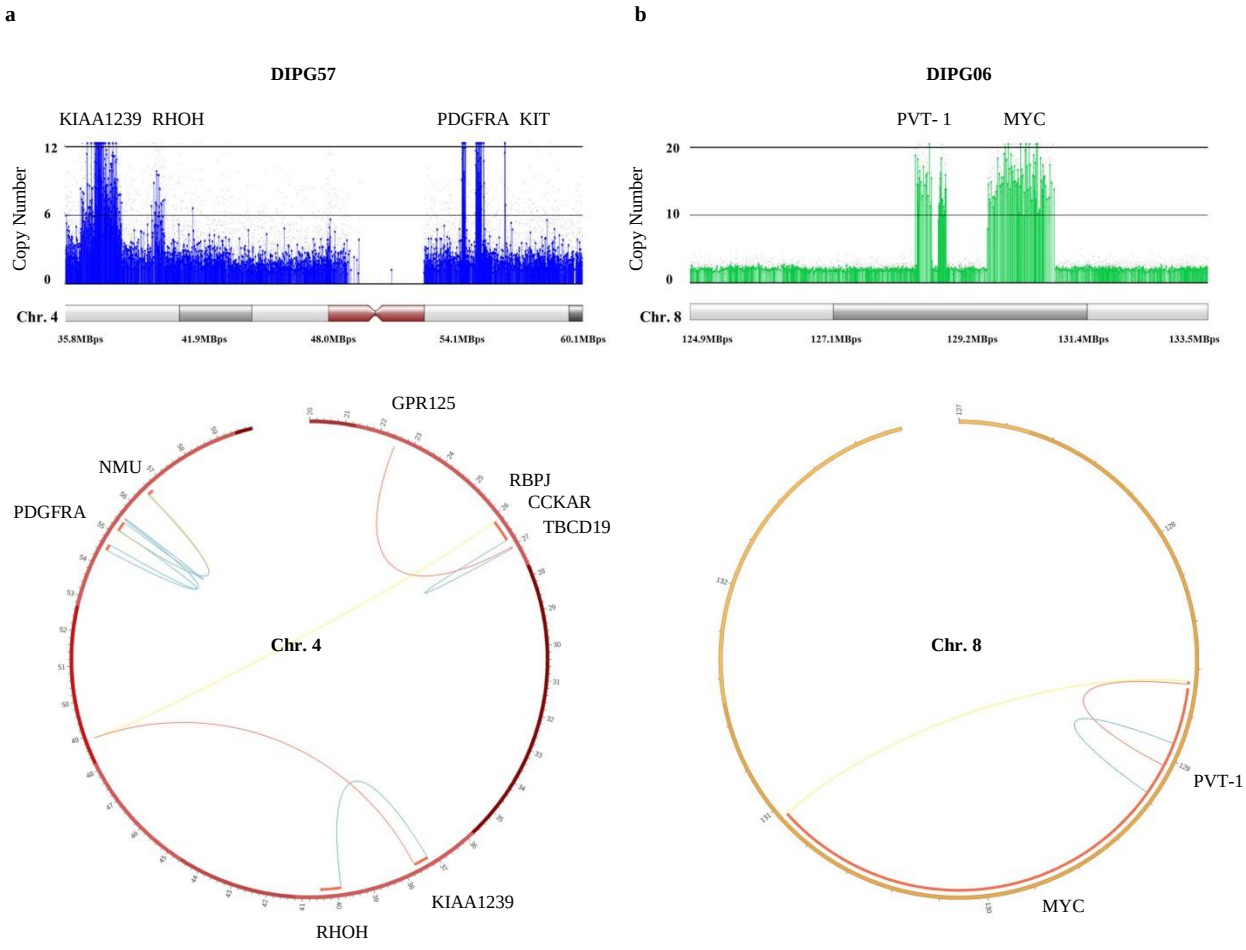

Supplementary Figure 5 H3-H27M DIPG exhibit structural variants in *PDGFRA* and *PVT-1/MYC* loci. H3-K27M DIPG patient often show gains and amplifications as well as structural variants in (a) *PDGFRA* and (b) *PVT-1/MYC*.

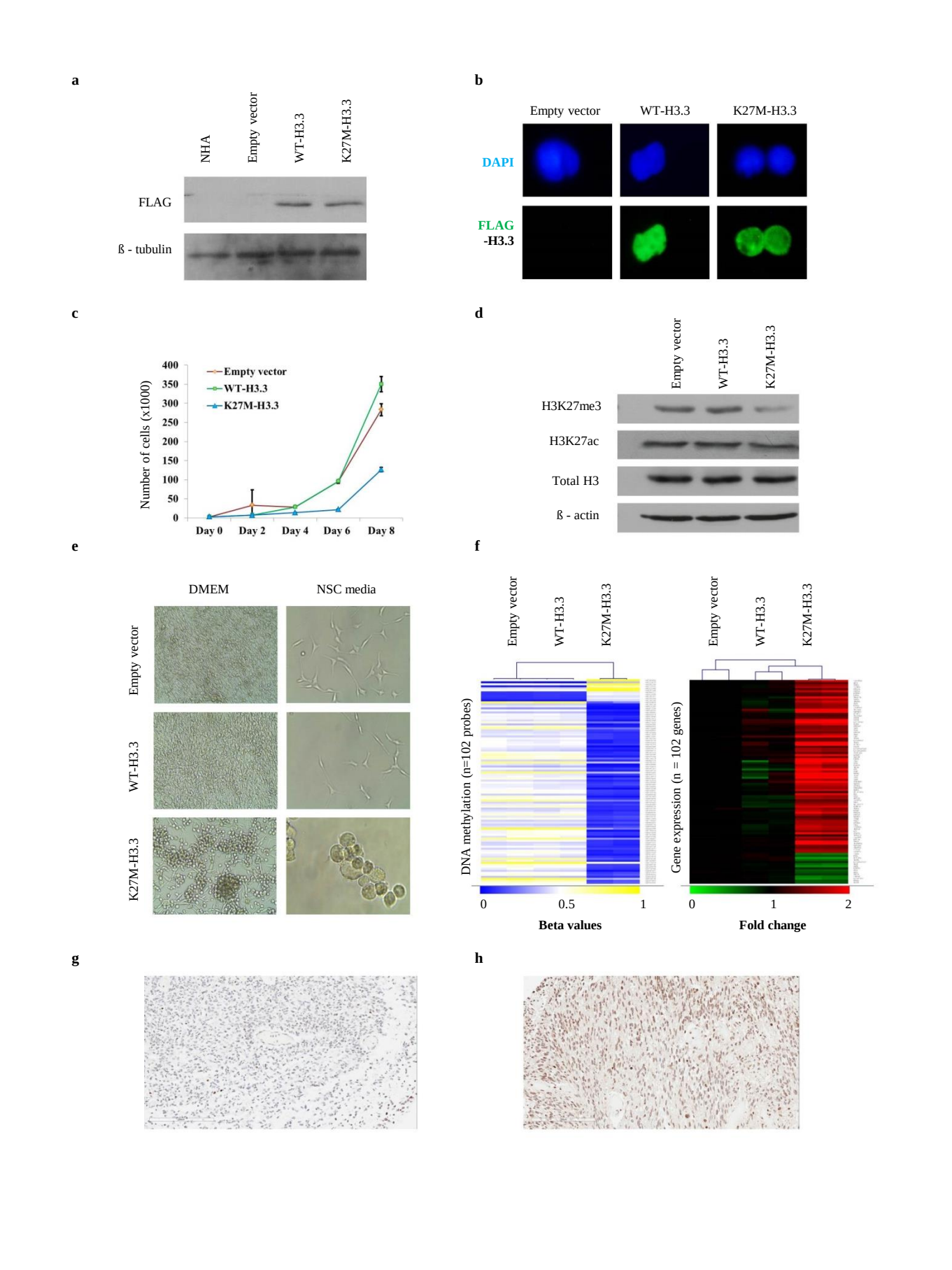
a
NHA
Empty vector
WT-H3.3
K27M-H3.3
FLAG
ß - tubulin
b
Empty vector
WT-H3.3
K27M-H3.3
DAPI
FLAG
-H3.3
c
Number of cells (x1000)
400
350
300
250
200
150
100
50
0
Empty vector
WT-H3.3
K27M-H3.3
Day 0
Day 2
Day 4
Day 6
Day 8
d
Empty vector
WT-H3.3
K27M-H3.3
H3K27me3
H3K27ac
Total H3
ß - actin
e
DMEM
NSC media
Empty vector
WT-H3.3
K27M-H3.3
f
Empty vector
WT-H3.3
K27M-H3.3
DNA methylation (n=102 probes)
0
0.5
1
Beta values
Empty vector
WT-H3.3
K27M-H3.3
Gene expression (n = 102 genes)
0
1
2
Fold change
g
h

Supplementary Figure 6 K27M-H3.3 exhibits global decrease in H3K27me3 when compared to WT-H3.3 *in vitro* and *in vivo.* (a) Western blot of FLAG-tagged WT-H3.3 and K27M-H3.3 reveals both clones expressing similar levels of protein. No expression was detected in untransfected NHA and NHA transfected with empty vector control. (b) Immunofluorescence staining of NHA shows nuclear localization of FLAG-tagged WT-H3.3 and K27M-H3.3 protein. (c) K27M-H3.3 expressing NHA cells have a decreased growth rate as compared to both WT-H3.3 and empty vector control ($p < 0.0001$). (d) By Western blot, H3K27me3 is decreased in K27M-H3.3 NHA as compared to WT-H3.3 and empty vector NHA cells by 52% ($p = 0.01$). (e) Immortalized NHAs transfected with K27M-H3.3 show phenotypic changes compared to empty vector and WT-H3.3 control, forming cell clusters at high density when seeded in DMEM and growing semi-adherently in neural stem cell media. (f) K27M-H3.3 NHAs have different methylation and expression profiles as compared to controls. The association of decreased H3K27me3 and mutant histone H3 is also seen by immunohistochemical staining of DIPG tissue micro-array, where patients with K27M-H3.3 (g) show decreased H3K27me3. DIPG patients that are WT-H3.3 (h) show more positive staining by IHC for H3K27me3.

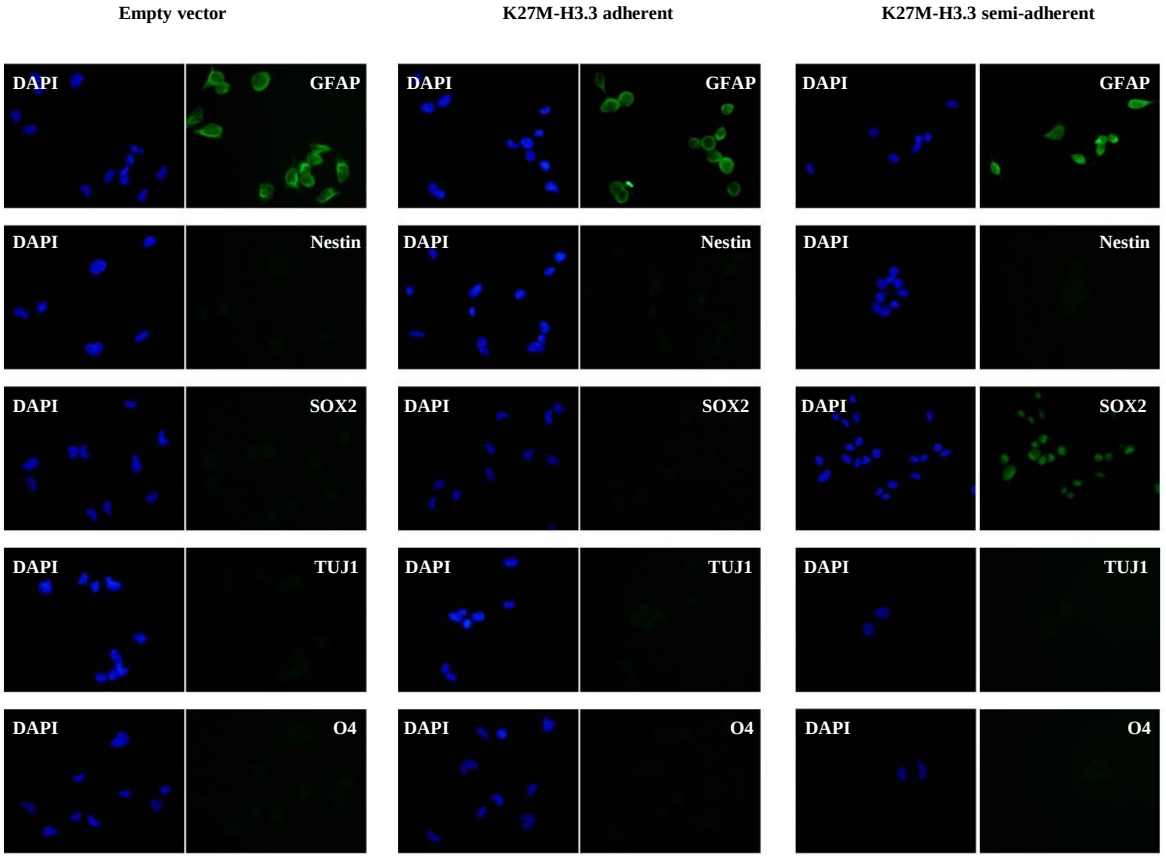

Supplementary Figure 7 K27M-H3.3 semi-adherent cells exhibit higher SOX2 expression. Immunofluorescence staining of empty vector, K27M-H3.3 adherent and K27M-H3.3 semi-adherent iNHA reveals increased SOX2 expression in the semi-adherent cells but no changes in GFAP, Nestin, TUJ1 or O4. Images were taken at 400X magnification.

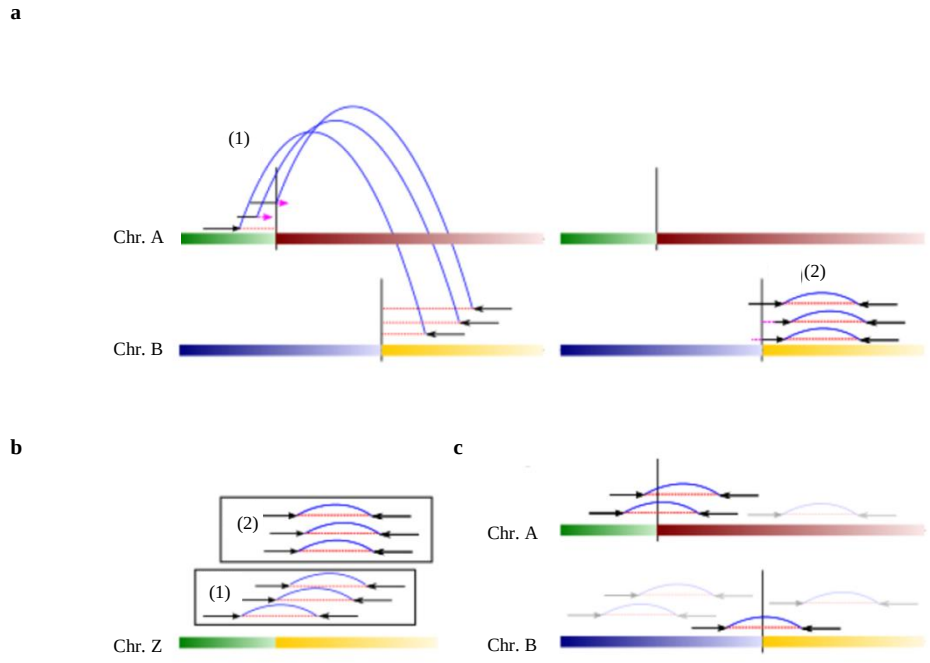

Supplementary Figure 8 Discordant read-pair clustering. (a) Schematic of discordant read pairs supporting a translocation event (1) and clipped mappings narrowing in breakpoint location (2). (b) Read-pairs as viewed by translocated region aligned to tumor genome. (c) The spanning reads in the normal sample provide an expected arrival count for the Poisson distribution when used to determine maximum likelihood copy counts.

Supplementary Table 5- WNT pathway genes over-expressed in Silent group DIPGs

Column ID	Fold-Chage (vs non-Silent)	p-value(vs non-Silent)
DVL1	2.1	0.043
FZD7	2.2	0.036
HOXB9	1.6	0.050
MARK2	2.0	0.038
MDM2	7.6	0.044
SDC1	2.8	0.045
SOX14	1.8	0.014
SOX17	2.0	0.049
TCF7L2	1.9	0.034
WNT10A	2.0	0.020
WNT16	1.5	0.044
WNT4	1.4	0.035
WNT7A	2.3	0.033

Supplementary Table 6- URLs

Bioinformatics Tool	URL
PicardTools 1.77	http://picard.sourceforge.net
MutSig	https://confluence.broadinstitute.org/display/CGATools/MutSig

Supplementary Table 8- Primer Sequences

Target	Forward Primer	Reverse Primer
K27M-H3F3A	ATAAAGCTTGCTCGTACAAAGCAGAC	TATGCGGCCGCTTAAGCACGTTCTCC
G238V-ACVR1	TTTGGGACCCAAGTGAAACCAGCCATT	AATGGCTGGTTTCACTTGGGTCCCAAA
ID1	TTGGAGCTGAACTCGGAATC	ATCGTCCGCAGGAACGCATG
ID2	CGCTGACCACCCTCAACAC	CAGCCACACAGTGCTTTGC
ACVR1	TATTTGGGCCTTTGGACTTG	CGGGTCTGAGAACCATCTGT
TBPF	TTCGGAGAGTTCTGGGATTG	GAAAATCAGTGCCGTGGTTC